

Characterization of a Highly Photoactive Molecular Semiconductor: Oxotitanium Phthalocyanine

Ph. Ghosez,[†] R. Côté, L. Gastonguay, G. Veilleux, G. Denès,[‡] and J. P. Dodelet*

INRS-Energie et Matériaux, C.P. 1020, Varennes, Québec, Canada J3X 1S2

Received June 18, 1993. Revised Manuscript Received August 16, 1993*

Oxotitanium phthalocyanine (OTiPc) thin films have been sublimed at various thicknesses on SnO₂ and glass substrates. The morphology, crystallinity, and photoelectrochemical activity of the films have been studied. It was found that the physical and photoelectrochemical properties of the films are greatly influenced by the temperature reached by the substrate during the sublimation. Below 80 °C, amorphous films are obtained while the films are partially crystalline when the substrate is allowed to reach about 140 °C. Amorphous films are made of tightly packed aggregates of circular section while partially crystalline films consists of platelets. All films are porous and permeable to the I₃⁻/I⁻ redox system. The dominant polymorph in partially crystalline films is not the same for all film thicknesses. It is phase IV OTiPc (as deduced by electron diffraction) for films thinner than about 2000 Å. On the other hand, for films thicker than about 8000 Å, phase I OTiPc becomes the dominant polymorph (as deduced by X-ray diffraction). It is replaced by phase II for 20 000-Å-thick films of OTiPc. Partially crystalline films are the only ones to absorb in the near-infrared (NIR) region. This typical absorption is going along with an improvement of the photoactivity of the films. In partially crystalline films, energy is transferred from the amorphous to the crystalline regions where most of the charges are generated. Quantum yields for electron collection per incident photon may reach over 25% in short circuit conditions, at 850 nm, the Q-band absorption maximum for 8000-Å-thick films. Those films are phase I OTiPc. Under 35 mW cm⁻² polychromatic illumination, the same films are characterized by short circuit photocurrents of 1.5 mA cm⁻². A NIR absorbance is an important factor required to obtain a high photoactivity, but it is not the only one. Interaction of OTiPc with oxygen at the purification level of the crude material is very important as well.

Introduction

Since their fortuitous discovery in 1907 by Braun and Tcherniac, phthalocyanines (Pcs) have become a major pigment in the dye industry. This material is also involved in high-technology applications. Indeed, since the mid sixties, the photoelectrical properties of phthalocyanines have attracted a lot of interest. They are progressively replacing Se as charge carrier generating layers in the photocopying process.^{1,2} More recently, they have also been used extensively to generate charges in the laser/light emitting diode printing process. For the new generation of diode-laser printers the photoconductors have to match the output of these devices. This occurs in the near infrared (NIR) at wavelength between 750 and 850 nm. It is a spectral region where some phthalocyanines were found to absorb intensively after ball milling, heating, changing of sublimation rate, or treating in organic solvents or aqueous electrolyte solution. These phthalocyanines are for instance α -H₂Pc,³ τ -H₂Pc,⁴ ϵ -CuPc,⁵ ClInPc,⁶ MgPc,⁷

ClAlPc,^{7,8} ClAlPcCl,⁹ ClGaPc,¹⁰ and OVPc.¹¹ Oxotitanium phthalocyanine (OTiPc) is also absorbing in the NIR. This material has been particularly considered since a highly sensitive polymorph has been reported.¹²⁻¹⁵

From the literature it is also common knowledge that NIR absorbing phthalocyanines are metastable but they are more photoactive than other more stable polymorphs of the same material. For instance, the quantum generation efficiency for the photogeneration of holes has been compared for α -, β -, x -, and τ -H₂Pc. At the same applied field, it is found that x - or τ -H₂Pc are about 10 times more photoactive than α - or β -H₂Pc.¹⁶ Similarly, it has been demonstrated photoelectrochemically, that ClGaPc molecules assembled to form a slipped-stack arrangement

[†] Present address: UCPM, Université Catholique de Louvain, Place Croix du Sud 1, 1348 Louvain-la-Neuve, Belgium.

[‡] Chemistry Department, Concordia University, Montréal, Québec Canada H3G 1M8.

* Abstract published in *Advance ACS Abstracts*, October 1, 1993.

(1) Gregory, P. In *High-Technology Application of Organic Colorants*; Plenum Press: New York, 1991; p 59.

(2) Loutfy, R. O.; Hor, A. M.; Hsiao, C. K.; Baranyi, G.; Kazmaier, P. *Pure Appl. Chem.* 1988, 60, 1047.

(3) Sharp, J. H.; Lardon, M. *J. Phys. Chem.* 1968, 72, 3230.

(4) Enokida, T.; Hirohashi, R.; Mizukami, S. *J. Imaging Sci.* 1991, 35, 235.

(5) Lee, S. N.; Hoshino, K.; Kokado, H. *Denshi Shashin Gakkaishi* 1992, 31, 2.

(6) Loutfy, R. O.; Hor, A. M.; Rucklidge, A. *J. Imaging Sci.* 1987, 31, 31.

(7) Loutfy, R. O.; Hor, A. M.; DiPaola-Baranyi, G.; Hsiao, C. K. *J. Imaging Sci.* 1985, 29, 116.

(8) Gastonguay, L.; Veilleux, G.; Côté, R.; Saint-Jacques, R. G.; Dodelet, J. P. *J. Electrochem. Soc.* 1992, 139, 337.

(9) Arishima, K.; Hiratsuka, H.; Tate, A.; Okada, T. *Appl. Phys. Lett.* 1982, 40, 279.

(10) Sims, T. D.; Pemberton, J. E.; Lee, P.; Armstrong, N. R. *Chem. Mater.* 1989, 1, 26.

(11) Griffiths, C. H.; Walker, M. S.; Goldstein, P. *Mol. Cryst. Liq. Cryst.* 1976, 33, 149.

(12) Enokida, T.; Hirohashi, R.; Nakamura, T. *J. Imaging Sci.* 1990, 34, 234.

(13) Hor, A. M.; Popovic, Z. In *Proc. 7th. Intl. Cong. on Adv. in Non Impact Printing Techn.* 1991, 1, 293.

(14) Tanako, S.; Mimura, Y.; Matsui, N.; Utsugi, K.; Gotoh, T.; Tani, C.; Tateishi, K.; Ohde, N. *J. Imaging Technol.* 1991, 17, 46.

(15) Fujimaki, Y.; Tadokoro, H.; Oda, Y.; Yoshioka, H.; Homma, T.; Moriguchi, H.; Watanabe, K.; Konishita, A.; Hirose, N.; Itami, A.; Ikeuchi, S. *J. Imaging Technol.* 1991, 17, 202.

(16) Kanemitsu, Y.; Yamamoto, A.; Funuda, H.; Masumoto, Y. *J. Appl. Phys.* 1991, 69, 7333.

Table I. Elemental Analysis of Sublimed OTiPc (in wt %)

element	theor value	exptl value
C	66.68	67.11
N	2.80	2.77
H	19.44	19.58
O	2.78	2.33
Ti ^a	8.31	8.25
Cl ^a	0	50 ppm

^a From neutron activation analysis.

absorbing in the NIR are more photoactive by a factor of at least 10 compared with ClGaPc molecules cofacially stacked in a linear assembly that absorbs only in the visible.¹⁰

Since OTiPc is one of the leading phthalocyanines in electrophotography, it is interesting to study some parameters that may govern its high photoactivity. This is done in this work by analyzing the morphology, the structure, and the photoelectrochemical properties of thin films of the pigment in regenerative cells using I₃⁻/I⁻ as a redox system. The following will be shown: (i) an absorbance in the NIR is essential but not the unique criterion to obtain a large photoactivity; oxygen doping also plays a major role. (ii) Amorphous or polycrystalline OTiPc can be obtained depending upon the substrate temperature. The amorphous to polycrystalline change has a large effect on the film photoactivity. (iii) The dominant OTiPc polymorph varies with the thickness of the film. However, large differences in the photoactivity are not observed between the various polymorphs of OTiPc.

Experimental Section

Synthesis and Purification. The synthesis of OTiPc has been performed according to a method inspired from Block and Meloni.¹⁷ The synthesis proceeds in two steps: (1) The synthesis of Cl₂TiPc (from 15.2 g of phthalonitrile + 9.4 g of TiCl₃ in 300 mL of chloronaphthalene + 80 mL of benzene, in N₂ ambient, at 250 °C; the crude Cl₂TiPc is filtered under N₂, washed with benzene, and dried under vacuum (~10⁻² Torr). (2) The hydrolysis of crude Cl₂TiPc (from 2 g of Cl₂TiPc, 1 mL of triethylamine refluxed in either 150 mL of ethanol 95%/water 5% (vol) or pyridine 80%/NH₄OH 20% (vol); the latter solvent is preferred for complete hydrolysis. The crude OTiPc is washed with methanol and with water before being dried under vacuum (~10⁻² Torr)).

The crude OTiPc is purified by two sublimations under vacuum in a long tube closed at one end. The material to be purified is loaded in the tube and maintained near the closed end by a glass wool plug. Half the length of the tube is inserted in a tubular furnace heated at 480–500 °C. The sublimed phthalocyanine crystallizes on the tube wall, just outside of the furnace. More volatile impurities spread on colder portions of the tube or get frozen in the liquid nitrogen traps. After sublimation, the tube is cut open and the well crystallized blue ring is collected.

In this work, the crude OTiPc has been sublimed at two different levels of vacuum (either ~10⁻² Torr, obtained with a roughing pump or ≤10⁻⁵ Torr obtained with a turbomolecular pump).

Elemental analyses have been performed on the purified OTiPc (sublimed at ~10⁻² Torr). They are reported in Table I. Values for C, H, N, and O have been obtained from Galbraith Laboratories and values for Ti and Cl have been obtained from neutron activation analysis (Ecole Polytechnique, Université de Montréal). As can be seen from Table I, the chlorine content of OTiPc is very low indicating a nearly complete hydrolysis of Cl₂TiPc.

Film Preparation. Films of OTiPc for photoelectrochemical measurements have been obtained by sublimation under vacuum

(≤10⁻⁵ Torr) on glass substrates covered with a transparent and conducting ($\rho_s = 25\text{--}30 \Omega \text{sq}^{-1}$) layer of SnO₂. Before sublimation, the substrates are first degreased with methanol, then they are immersed during 30 min in a sulfochromic cleaning solution, rinsed with deionized water and dried under a flow of N₂. The substrates are then mounted on the rotating support in the sublimation unit.

Six pairs of films can be prepared without breaking the vacuum. For film deposition, each pair of substrates is brought at the vertical of the crucible situated in a glass tube at about 11 cm under the substrates. To avoid possible contamination by Pc decomposition products, the heat source is not in the vacuum system but outside around the glass tube containing the crucible. The rate of sublimation is controlled by adjusting the crucible temperature. The substrate temperature is not controlled. This is not important when the substrates remain above the crucible for short periods of time (≤2 min). However, in this work, deposition times up to 30 min have been used. In these conditions, the substrate temperature may drift away from room temperature as it will be seen in the result section.

Film thicknesses have been measured by profilometry (Dektak 3030) for films thicker than 2000 Å. Since profilometry is not accurate for thinner films, their thickness was deduced from their absorbance at 705 nm. A 2000-Å-thick film has an absorbance of 4.0 at 705 nm. The linear absorption coefficient of OTiPc at 705 nm is therefore 2 × 10⁶ cm⁻¹. It was used to estimate the thickness of films thinner than 2000 Å and characterized by the same absorption spectrum. Using an absorbance of 4.0 as reference for a 2000-Å-thick film might lead to some inaccuracy in film thickness determination since the transmitted light is 10⁴ smaller than the incident one. However, cross-checking with films slightly thicker than 2000 Å at wavelengths where the pigment is less absorbing yielded a good agreement between the thickness values deduced by profilometry and by absorbance.

Measurements. The electrochemical measurement setup has already been described in ref 8. Briefly, a three-electrode, one-compartment cell was used. The electrolyte was I₃⁻/I⁻ (0.005 M/0.4 M) at pH 3. $E_{\text{redox}} = 0.264 \text{ V vs SCE}$. It was bubbled with Ar mainly to get rid of diffusion problems of the redox species. Polychromatic illumination was obtained from a high-pressure 450-W Xe lamp light beam passing through a 385-nm cut-on UV filter and a 10-cm water filter. The white light power was measured with a Scientific 362 (thermocouple-based) power meter. At the sample, the white light power is 35 mW cm⁻² unless otherwise specified. Monochromatic illumination for action spectra was performed with a 650-W tungsten halogen lamp and a Schoffel Instruments monochromator. Light intensities were measured by a coherent 212 (Si diode based) power meter. Action spectra were recorded under short circuit conditions. All currents were normalized at an incident photon flux of 9.7 × 10¹⁴ photons cm⁻² s⁻¹ for all wavelengths, using a linear dependence of the short-circuit photocurrent vs the photon flux. It is correct in the range of intensities used.

Film morphologies were investigated by scanning electron microscope (SEM). The OTiPc layers were covered with a thin Au film in order to avoid charging problems.

Structural information was obtained from electron diffraction measurements according to a procedure described in ref 8. Films for transmission electron microscopy (TEM) were sublimed onto glass slides precoated with a thin gold layer. The films were lifted from their glass support by corroding the gold layer with an I₃⁻/I⁻ solution of the same composition than the one used for photoelectrochemical measurements. The floating OTiPc was recovered onto suitable TEM grids.

X-ray diffraction (XRD) were obtained from OTiPc films and powder according to a procedure described in ref 18.

Results and Discussion

(I) Effect of Oxygen on the Photoactivity of OTiPc. Figure 1 displays the short-circuit photocurrent, J_{SC} , under

(17) Block, B. P.; Meloni, E. G. *Inorg. Chem.* **1965**, *4*, 111.

(18) Côté, R.; Denès, G.; Gastonguay, L.; Dodelet, J. P. *Proc. SPIE—Int. Soc. Opt. Eng. (Photovoltaics, Photochem. Photoelectrochem.)* **1992**, *1729*, 222.

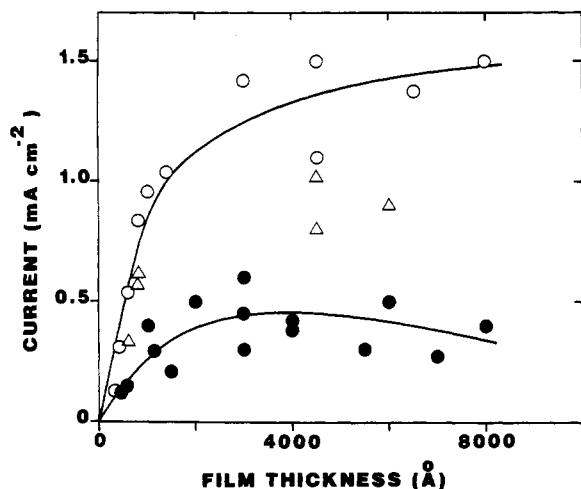


Figure 1. Short-circuit photocurrents, J_{sc} , of OTiPc films of various thicknesses; OTiPc powder has been sublimed in 10^{-2} Torr (O) or in $\leq 10^{-5}$ Torr (●); Δ, OTiPc powder has been sublimed in $\leq 10^{-5}$ Torr then heated in 1 atm of O_2 .

polychromatic illumination (35 mW cm^{-2}) of OTiPc films of various thicknesses sublimed at 360°C on SnO_2 . The open points represent films obtained from OTiPc powder purified by two successive sublimations under a vacuum of about 10^{-2} Torr, while the same crude OTiPc powder, purified by two successive sublimations under a vacuum of $\leq 10^{-5}$ Torr, give the J_{sc} curve represented by the dark points in Figure 1.

To demonstrate that the large difference in the photoactivity of the pigment is due to the amount of oxygen present during the purification step of the crude OTiPc and not to some impurities introduced during the synthesis, the following experiments were performed:

(1) The synthesis procedure of OTiPc was slightly modified. The modifications involved a change of solvents (naphthalene instead of chloronaphthalene in the preparation of Cl_2TiPc or pyridine/ NH_4OH instead of ethanol/water for the hydrolysis of Cl_2TiPc). When these pigments were purified under a vacuum of 10^{-5} Torr, they all produced films of about the same photoactivity (dark points in Figure 1) indicating that modifying the synthesis procedure does not affect the photoactivity of the film.

(2) OTiPc powder, purified under a vacuum of 10^{-5} Torr, was heated during 60 h at 130°C in pure O_2 at 1 atm. Films sublimed from that powder, in the same conditions as those prevailing in Figure 1, showed an improved photoactivity. They are reported as Δ symbols in Figure 1. The effect of O_2 on the photoactivity of OTiPc is however lower than for OTiPc purified under low-vacuum conditions (10^{-2} Torr). In the latter case, more oxygen interacts with individual molecules during sublimation while in the process of heating an already sublimed powder under an oxygen flow, O_2 has to diffuse between the grains of the crystalline structure and eventually into the bulk of the material.

The effect of oxygen on the dark conductivity and on the photoconductivity of phthalocyanines is well documented. The formation of the complex Pc^+O_2^- is responsible for their p-type semiconductor character. In the presence of O_2 , the dark conductivity of Pcs increases and its activation energy decreases.¹⁹⁻²² The easier carrier

generation arises from the small size of oxygen relative to Pc. The electron polarization energy, P^- , associated with a species such as O_2^- is substantially larger than that for a species such as Pc^- . The energy for charge carrier generation in molecular semiconductors is $\text{IP}-\text{EA}-\text{P}^+-\text{P}^-$, where IP, EA, and P^+ are the ionization potential, the electron affinity, and the hole polarization energies, respectively.²³ An increase in P^- will therefore reduce the conduction activation energy even if there is no associated electron affinity difference.²⁴

Oxygen adsorbs at the surface of the material and/or diffuses deeply into its bulk resulting in the emergence of electron traps releasing holes which are the majority carriers.^{22,25-32} There is usually more than one adsorption site for O_2 ,^{30,33-35} for instance, adsorbed H_2O derived species were found essential for the reversible O_2 uptake in PbPc. This has been demonstrated by X-ray photoelectron spectroscopy (XPS).^{36,37} In that material O_2^-/OH surface complexes are necessary to promote bulk O_2^- formation.

The presence of Pc^+O_2^- , especially on the surface of the material is also beneficial to the photoconductivity of the Pcs.²⁴⁻²⁶ Their local electric field induces exciton dissociation into free ions. In the extrinsic photogeneration mechanism proposed by Popovic,³⁸ O_2^- could play the role of the negative impurity, whose electron is excited by an exciton into the host conduction band and is regenerated by the thermal excitation of an electron from the valence band where a hole appears.

The role of gaseous O_2 dopant on the photoelectrochemical response of films of ClGaPc has been studied in detail by Armstrong's team.³⁹ They report that high-temperature O_2 doping of ClGaPc (48 h at 140°C in pure O_2 at atmospheric pressure) can turn a film that behaves like a lightly doped semiconductor into a p-type material while a similar treatment on OVPc and OTiPc results in no appreciable change in their photoelectrochemical properties. It is supposed that the barrier density of these pigments is already above 10^{18} cm^{-3} . XPS studies⁴⁰ of OVPc sublimed at 5×10^{-10} Torr on Au showed one O_{1s} peak at 531.8 eV with an O/V ratio of 1. It corresponds to the oxygen in the $\text{V}=\text{O}$ bond. However, when the OVPc

- (20) Collins, R. A.; Mohammed, K. A. *J. Phys. D: Appl. Phys.* 1988, 21, 154.
 (21) Martin, M.; André, J. J.; Simon, J. *J. Appl. Phys.* 1983, 54, 2792.
 (22) Dahlberg, S. C.; Musser, M. E. *J. Chem. Phys.* 1980, 72, 6706.
 (23) Lyons, L. E. *J. Chem. Soc.* 1957, 5001.
 (24) Wright, J. D. *Prog. Surf. Sci.* 1989, 31, 1.
 (25) Day, P.; Price, M. G. *J. Chem. Soc. A* 1969, 236.
 (26) Saito, T.; Kawanishi, T.; Kakuta, A. *Jpn. J. Appl. Phys.* 1991, 30, L1182.
 (27) Bahra, G. S.; Chadwick, A. V.; Couves, J. W.; Wright, J. D. *J. Chem. Soc., Faraday Trans 1* 1989, 85, 1979.
 (28) Couves, J. W.; Tamizi, M.; Wright, J. D. *J. Chem. Soc., Faraday Trans. 1990, 86, 115.*
 (29) Yasunaga, H.; Kojima, K.; Yohda, H.; Takeya, K. *J. Phys. Soc. Jpn.* 1974, 37, 1024.
 (30) Hassan, A. K.; Gould, R. D. *J. Phys. Condens. Matter* 1989, 1, 6679.
 (31) Pack, J. L.; Phelps, A. V. *J. Chem. Phys.* 1966, 44, 1870.
 (32) Hassan, A. K.; Gould, R. D. *Int. J. Electronics* 1990, 69, 11.
 (33) Waite, S.; Pankow, J.; Collins, G.; Lee, P.; Armstrong, N. R. *Langmuir* 1989, 5, 797.
 (34) Musser, M. E.; Dahlberg, S. C. *Surf. Sci.* 1980, 100, 605.
 (35) Wilson, A.; Collins, R. A. *Phys. Status Solidi A* 1986, 98, 633.
 (36) Archer, P. B. M.; Chadwick, A. V.; Miasik, J. J.; Tamizi, M.; Wright, J. D. *Sensors Actuators* 1989, 16, 379.
 (37) Mockert, H.; Schmeisser, D.; Göpel, W. *Sensors Actuators* 1989, 19, 159.
 (38) Popovic, Z. D. *J. Chem. Phys.* 1982, 77, 498.
 (39) Klofta, T. J.; Sims, T. D.; Pankow, J. W.; Danziger, J.; Nebesny, K. W.; Armstrong, N. R. *J. Phys. Chem.* 1987, 91, 5651.
 (40) Klofta, T. J.; Danziger, J.; Lee, P.; Pankow, J.; Nebesny, K. W.; Armstrong, N. R. *J. Phys. Chem.* 1987, 91, 5646.

(19) van Ewyk, R. L.; Chadwick, A. V.; Wright, J. D. *J. Chem. Soc., Faraday Trans. 1* 1980, 76, 2194.

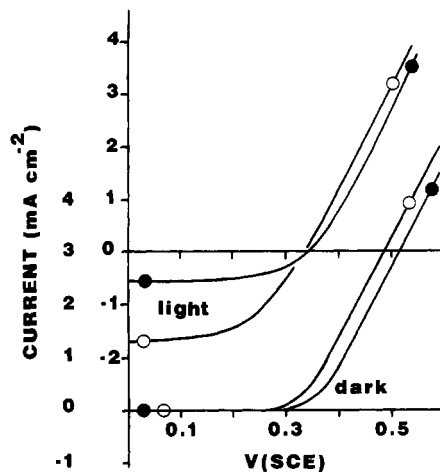


Figure 2. Comparison of J - V curves obtained in the dark or under illumination of two 4000-Å-thick films; both films have been prepared from OTiPc powder purified by sublimations at 10^{-2} Torr (○) and at 10^{-5} Torr (●).

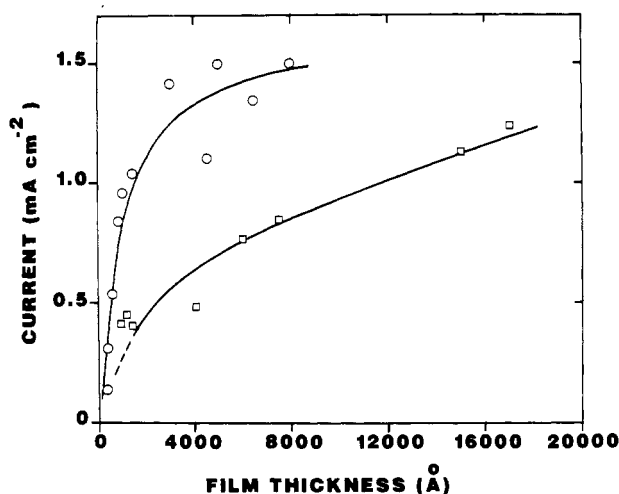


Figure 3. Evolution of the short circuit photocurrent, J_{sc} , as a function of the film thickness for two sublimation temperatures: 360 °C (○) and 400 °C (□).

film, sublimed at 5×10^{-10} Torr is exposed for 6 h at 148 °C to O_2 atmospheric pressure, another O_{1s} peak at 533.3 eV is observed. The latter peak does not appear if the film is not brought to high temperature. The new oxygen species has not been identified. Similar results are expected for OTiPc.

In the present work, changes in oxygen doping do not seem to modify the dark conductivity of the films. They only affect their photoconductivity. This can be observed in Figure 2, where J - V curves are presented in the dark and under illumination for two films of about the same thickness (4000 Å); both films have been prepared from OTiPc powder purified by sublimations at 10^{-2} Torr (○) and at $\leq 10^{-5}$ Torr (●), respectively. From the slope of the forward bias part of the curve, series resistance values of $51 \Omega \text{ cm}^2$ are obtained for both films in the dark. However, it is possible that the series resistance is limited by the SnO_2 substrate. The evolution of the carrier density and the variation of their mobility with oxygen doping is presently under study to understand the exact role of oxygen in these films.

Unless otherwise specified, the subsequent results and discussions only deal with films obtained from OTiPc powders purified by sublimation at about 10^{-2} Torr and characterized by a high photoactivity.

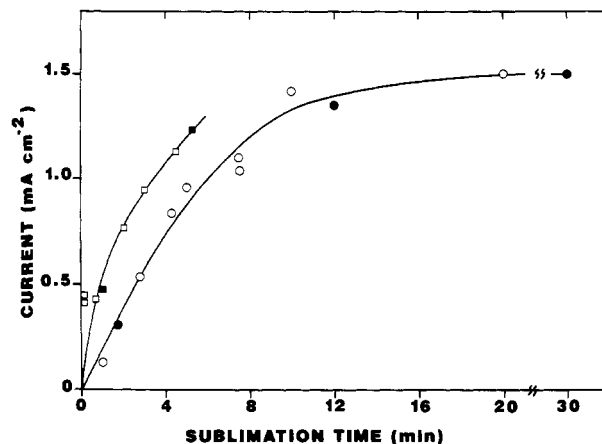


Figure 4. Evolution of the short circuit photocurrent, J_{sc} , as a function of the duration of the deposition, t , for two sublimation temperatures: 360 °C (○) and 400 °C (□). Dark symbols in the figure correspond to films whose morphology is illustrated in Figure 6.

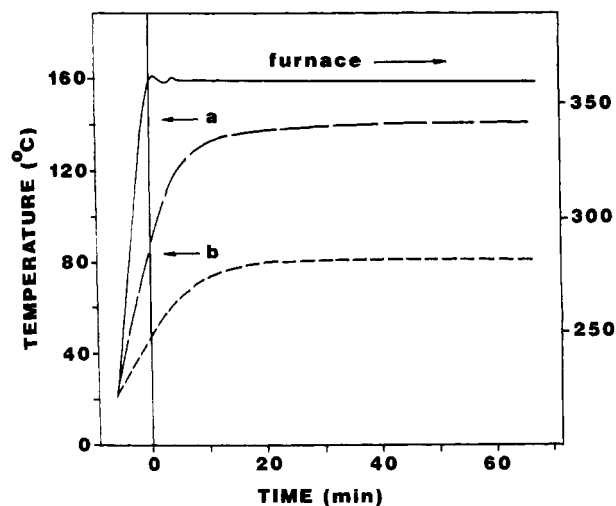


Figure 5. Time evolution of the substrate temperature for a sublimation at 360 °C; at the vertical of the heat source (a); in the waiting position, at an angle of 60° away from the heat source (b).

(II) Effect of the Substrate Temperature on the Photoactivity of OTiPc. Short-Circuit Photocurrents.

Figure 3 presents the evolution of the short circuit photocurrent density, J_{sc} , as a function of thickness of the film for two sublimation temperatures: 360 °C (○) and 400 °C (□). They correspond to sublimation rates of about 300 and 3000 Å min^{-1} , respectively. The power of the polychromatic illumination is 35 mW cm^{-2} . When both curves are compared, at the same J_{sc} value, one observes that a much larger film thickness (about 7 times) is required at the high sublimation rate (□) to obtain the same photocurrent as at low sublimation rate (○).

A different perspective is presented in Figure 4. The latter figure shows the evolution of J_{sc} vs deposition time for the same sublimation temperatures. In this graph, the two curves are brought closer together. It indicates, as seen later, that the duration of the deposition is a critical parameter in the photoactivity of OTiPc film.

In the Experimental Section, we stated that the substrate temperature was not controlled in the deposition system used. The substrate temperature increases during the deposition because the films are grown at the vertical of the heat source. Changes of substrate temperature are

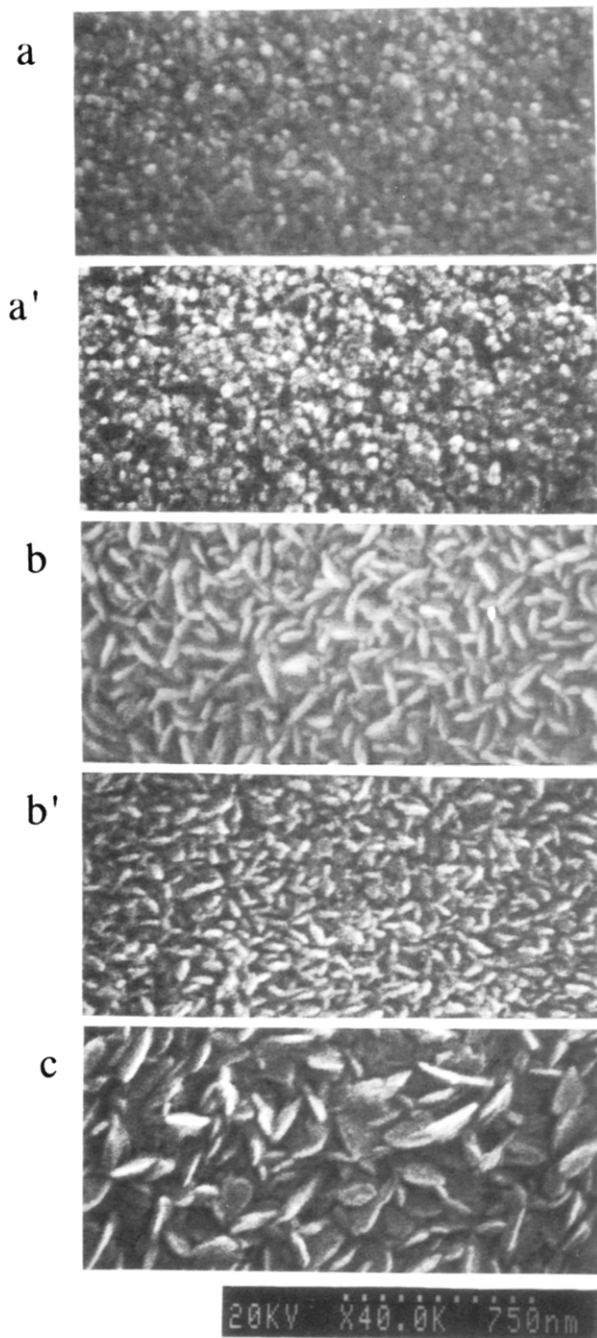


Figure 6. SEM micrographs of the morphology of OTiPc films represented by the dark symbols in Figure 4 for $J_{sc} = 0.4 \pm 0.1 \text{ mA cm}^{-2}$ (a and a'); $J_{sc} = 1.3 \pm 0.05 \text{ mA cm}^{-2}$ (b and b'); $J_{sc} = 1.5 \text{ mA cm}^{-2}$ (c).

presented in Figure 5 for two positions in the system during a sublimation at 360 °C. The origin of the time axis is set at the time required by the furnace to reach the sublimation temperature. Curves a and b depict the temperature evolution of a substrate placed, respectively, at the vertical of the heat source (a) and in the waiting position, at an angle of 60° away from the heat source, before switching the furnace on. One can see that if a film is grown during 15 min, its substrate reaches an equilibrium temperature of about 140 °C while the substrate in the waiting position reaches 80 °C. As it will be seen later, the increase of the substrate temperature during sublimation explains the behavior of Figure 4 and the SEM and TEM results that are the subject of the next section.

SEM and TEM Results. Figure 6a,a' shows SEM micrographs depicting the morphology of two OTiPc films

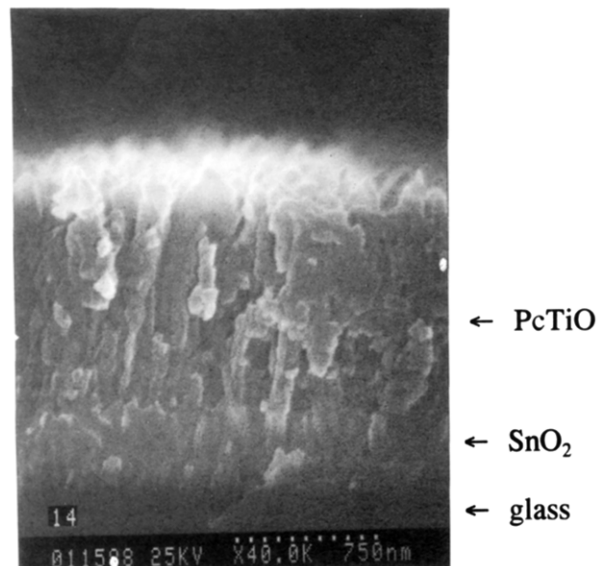


Figure 7. Cross section of a film displaying the same morphology as the one presented in Figure 6b or 6b'.

sublimed at 360 °C (a) and 400 °C (a'). They are characterized by a J_{sc} value of $0.4 \pm 0.1 \text{ mA cm}^{-2}$ and represented by the dark symbols in Figure 4 (●, 360 °C; ■, 400 °C). Similarly, Figure 6b,b' present films characterized by J_{sc} values of $1.3 \pm 0.5 \text{ mA cm}^{-2}$ in Figure 4. Figure 6c displays the morphology of a film sublimed at 360 °C during 30 min and characterized by the highest J_{sc} value: 1.5 mA cm^{-2} . From those figures, one may conclude that as the deposition time increases and as the temperature of the substrate rises, there is an evolution in the film morphology going along with an improvement of J_{sc} .

Parts a and a' of Figure 6 are very similar. They are made of tightly packed aggregates of circular section, having a diameter of about 500 Å. This morphology is characterized by a low J_{sc} values, independently of the sublimation temperature. At the highest J_{sc} value, the film is characterized by platelets (Figure 6c) similar to those already described by Sims et al.¹⁰ for OVPC. For the latter material, the platelet morphology is typical of molecules in a slipped stack arrangement leading to a red-shifted Q band in the NIR and a higher photoactivity (at least by a factor of 10) compared with the cofacial stacking. In the present case, the OTiPc films displaying a well defined platelet morphology are also characterized by the highest photoactivity. Parts b and b' of Figure 6 are also composed of platelets characterized by J_{sc} values ($1.3 \pm 0.5 \text{ mA cm}^{-2}$) intermediate between those of Figure 6a,c.

A cross section of a film displaying the same morphology as the one depicted in Figure 6b,b' is presented in Figure 7. It indicates that the film structure is dense and composed of elongated platelets growing perpendicular to the film surface. As the platelets appear homogeneous along their long axis, the annealing treatment resulting from the rise of the substrate temperature during the deposition alters therefore the structure of the entire film.

TEM experiments have been performed to determine the crystalline structure of the films. For TEM experiments, films must be thin in order to be transparent to the electron beam. Two films of 1300 Å have been prepared in the following conditions. The first one (○) has been sublimed in 3 min. During the sublimation, the substrate temperature rose from 48 to 80 °C. For the second film (S), the substrate has been left in the waiting position

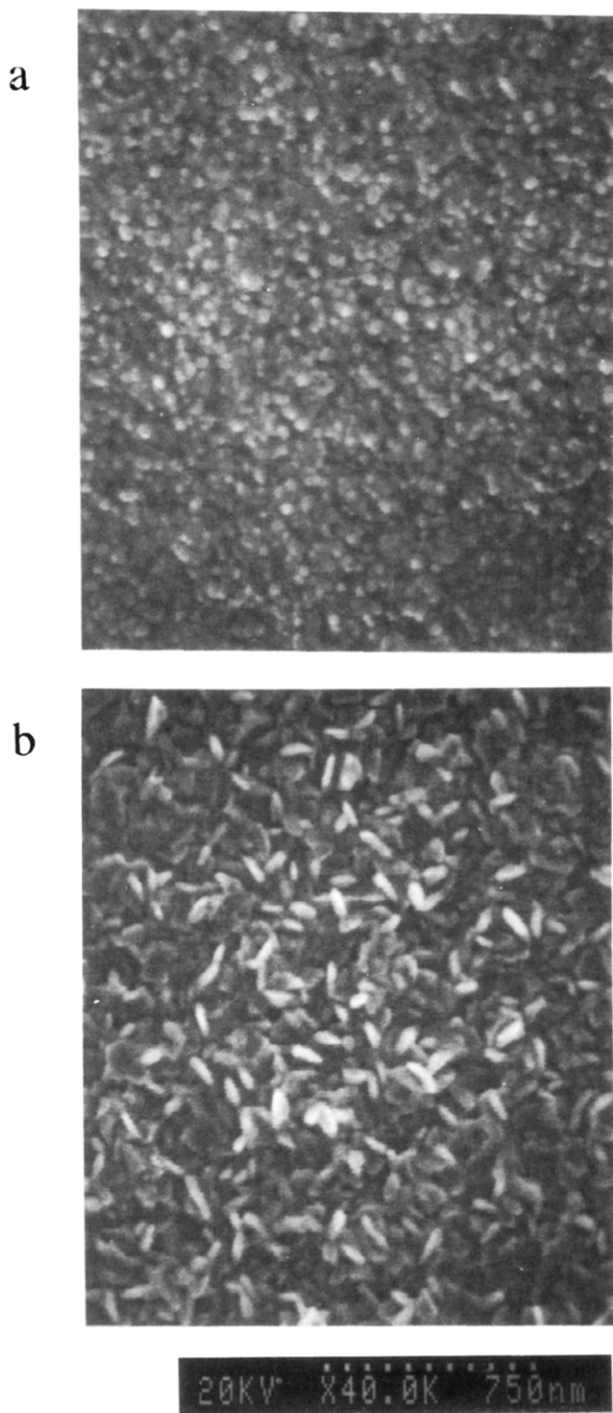


Figure 8. SEM micrographs of the morphology of two 1300-Å-thick films; during the sublimation, the substrate temperature rose from 48 to 80 °C (Q type film) (a); or from 80 to 132 °C (S type film) (b).

during 45 min; then it was brought in the sublimation position and left for 10 min. In these conditions, the substrate temperature rose from 80 to 132 °C during the sublimation. For both films, Q and S, the sublimation temperature was adjusted to obtain a thickness of 1300 Å in the experimental conditions described.

The morphology of Q and S films is depicted in parts a and b of Figure 8 respectively. One may conclude that Figure 8a is similar to both parts a and a' of Figure 6, while Figure 8b resembles Figure 6b,b'. Furthermore, the photocurrents obtained for Q and S are 0.34 and 0.95 mA cm⁻². They are in agreement with the relation J_{sc} film morphology mentioned previously.

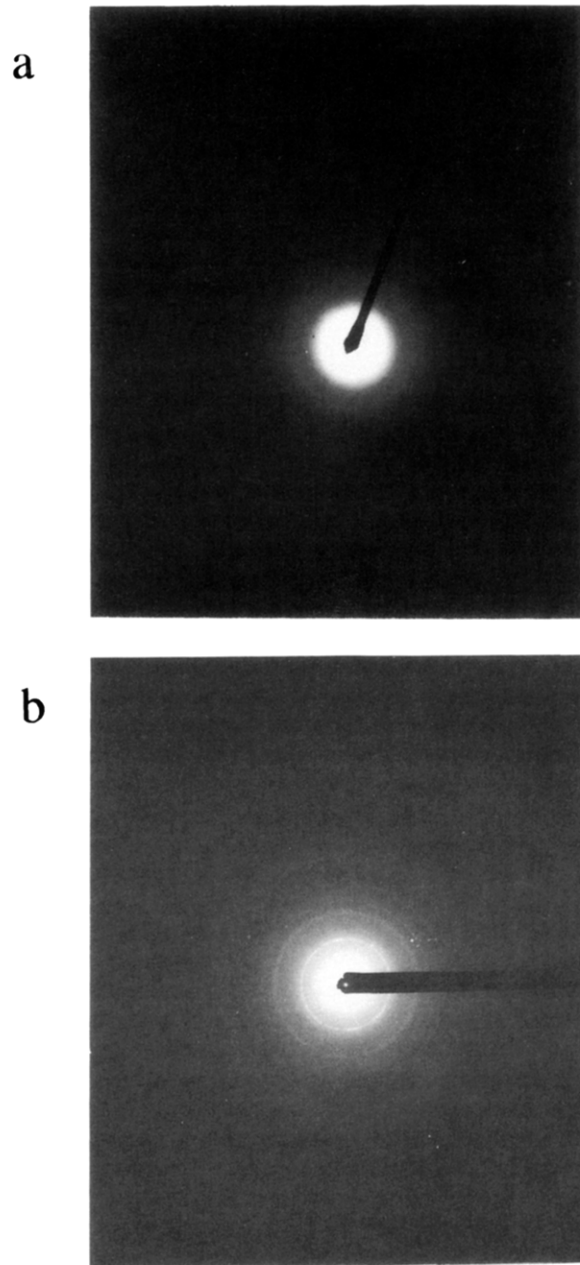


Figure 9. TEM electron diffraction of 1300-Å-thick films of the Q type (a) and on the S type (b).

TEM diffractograms of films Q and S are presented in parts a and b of Figure 9, respectively. From these figures, it appears that film Q is amorphous (or composed of molecules organized on very short range only) and that film S is crystalline with amorphous regions. The rather circular aggregates depicted in Figure 8a and Figure 6a,a' are therefore characteristic of an amorphous phase. A similar observation was made recently for ClAlPc.⁴¹

When the duration of the sublimation increases, the substrate temperature rises. It induces some crystallization of the amorphous phase and improves the photoactivity of the film.

It is however to be noticed that a platelet morphology is required but not sufficient to reach high photoactivities. This is demonstrated in Figure 10. It shows the morphology of a film obtained from OTiPc powder purified by sublimations of the crude material in a vacuum of $\leq 10^{-5}$

(41) Gastonguay, L.; Veilleux, G.; Côté, R.; Saint-Jacques, R. G.; Dodelet, J. P. *Chem. Mater.* 1993, 5, 381.

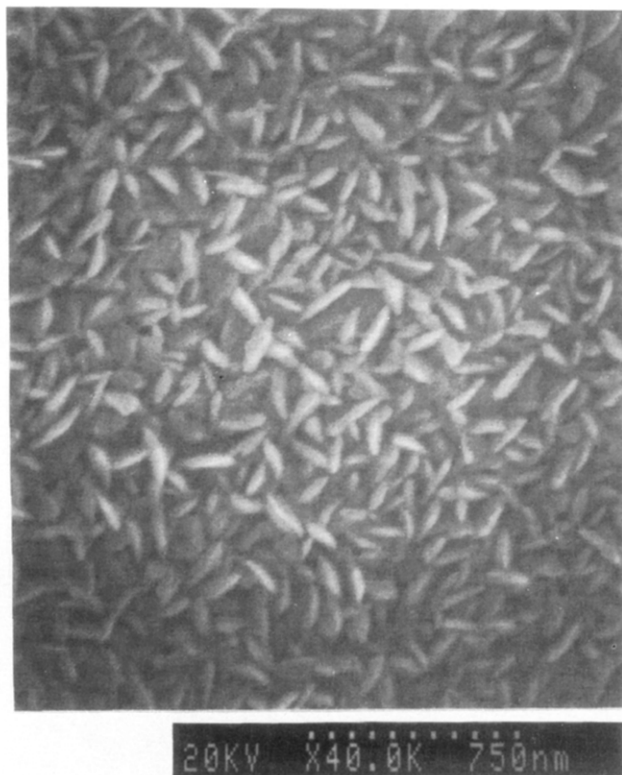


Figure 10. SEM micrograph of the morphology of a 4000-Å-thick OTiPc film belonging to the low J_{sc} value curve in Figure 1.

Torr. Although the film is grown during 20 min, up to a thickness of 4000 Å, and displays the typical morphology of a partially crystallized phase, it is only characterized by a J_{sc} value of 0.42 mA cm⁻² (Figure 1). Both morphology requirement + adequate oxygen doping are therefore needed to generate high photoactivities.

Experimental interplanar distances, d , of crystalline OTiPc can be deduced from the TEM diffraction pattern presented in Figure 9b. They are reported in Table II for d values above 3.5 Å. The largest d values are the most significant ones because they are representative of low index planes and could be used to identify the crystal structure of the material. The largest d values are obtained from the diffraction rings closest to the transmitted electron beam spot which is the center of all rings.

Table II also reports the calculated interplanar distances for the closest ($hk0$) planes of the four crystallographic phases reported for OTiPc. Phase I (also identified as β -OTiPc) crystallizes monoclinic in the space group $P2_1c$ with 4 molecules/unit cell.⁴² Phase II (also identified as α -OTiPc) crystallizes triclinic in the space group $P\bar{1}$ with 2 molecules/unit cell.⁴² The crystalline structure of phases I and II has been obtained from X-ray diffraction of single crystals and the lattice parameters are given in Table II. Phases IV and Y are metastable. Their crystalline structure has been deduced by Rietveld analysis of the X-ray powder diffraction patterns and the lattice parameters are given in Table II. Phase IV crystallizes triclinic in the space group $P\bar{1}$ with 2 molecules/unit cell.⁴³ Phase Y crystallizes monoclinic in the space group $P2_1c$ with 4 molecules/unit cell.⁴⁴

The stacking of the molecules has been reported for all four phases. From these reports, it seems that the plane of the macrocycles are always parallel to (or at a small angle with) the ab plane of the lattice. If we assume that the molecules are lying flat on the substrate, the only diffracting planes in TEM (tilt = 0°) are those characterized by a Miller index $l = 0$. Indeed, the only crystallographic planes diffracting electrons in TEM are those containing the electron beam or being at a small angle ($\leq 5^\circ$) with it. In our TEM setup, the electron beam is perpendicular to the substrate. It is also perpendicular to the plane of the macrocycles if the assumption made about the orientation of the molecules holds. This is a reasonable assumption because it has already been demonstrated⁴⁵ by X-ray absorption spectroscopy at the C and N edges that chloroaluminum phthalocyanine molecules are oriented with their macrocycle parallel to the substrate; chloroaluminum phthalocyanine and OTiPc are molecules of similar structure.

Table II reports $|\Delta d|$ = the absolute value of d (calculated) - d (experimental) and also $\Sigma|\Delta d|$ defined as the sum of all the differences between experimental interplanar distances and the closest calculated ones for a plane ($hk0$). From $\Sigma|\Delta d|$ for the various phases considered in Table II, one may conclude that the crystalline phase in OTiPc sublimed thin films is best described by phase IV of OTiPc known to be highly photoactive.¹³

When the thickness of the film increases, it becomes possible to obtain significant X-ray diffraction spectra. Table III reports 2θ values and relative intensities for films of various thicknesses (from 8 000 to 20 000 Å of OTiPc) sublimed on glass. It has been verified that the same peaks appear for films deposited on SnO₂. However, on the latter substrate, the diffractogram is complicated by the contribution of the SnO₂ polycrystalline layer to the diffraction.

All OTiPc polymorphic variations are commonly distinguished by their X-ray powder diffraction pattern. Phase IV is characterized by a main peak at 2θ (Cu K α) = 27.2°.^{13,43} The main peak for phase I is at $2\theta = 26.2^\circ$.^{14,43} There is also an intense diffraction at $2\theta = 13.1^\circ$. Phase II is characterized by broad peaks at $2\theta = 12.6, 24.3, 25.3,$ and 28.5° .^{14,43} From Table III, it can be seen that films of 8 000 to 13 000 Å thick are best characterized by phase I of OTiPc with a small contribution of phase II polymorph. For thicker films, the contribution of phase II becomes more important and even dominant for the thickest film.

From TEM and XRD results it seems therefore that the dominant polymorphic phase of OTiPc films, sublimed on SnO₂ in the conditions described in this work, varies from phase IV to phase I (the most stable one) to phase II, as the thickness of the film changes from ≤ 2 000 to 20 000 Å. For thin films, it is possible that phase IV, which is metastable, is stabilized by the interactions of the OTiPc first layer of molecules with the substrate. This interaction would fade away as the film thickness increases and structure defects accumulate.

Absorption and Action Spectra. Figure 11 presents the absorption spectrum of OTiPc in solution in chloronaphthalene. In accordance with the observations of Edwards and Gouterman,⁴⁶ the Q band is characterized

(42) Hiller, W.; Strähle, J.; Kobel, W.; Hanack, M. *Z. Kristallogr.* **1982**, *159*, 173.

(43) Bluhm, T.; Mayo, J.; Hamer, G.; Martin, T. *Proc. SPIE—Int. Soc. Opt. Eng. (Color Hard Copy Graphic Arts)* **1992**, *1670*, 160.

(44) Oka, K.; Okada, O.; Nakada, K. *Jpn. J. Appl. Phys.* **1992**, *31*, 2181.

(45) Guay, D.; Tourillon, G.; Gastonguay, L.; Dodelet, J. P.; Nebesny, K. W.; Armstrong, N. R.; Garrett, R. *J. Phys. Chem.* **1991**, *95*, 251.

Table II. Interplanar Distances, d (Å), of Diffracting (hkl) Planes for OTiPc Films

exptl d	phase I ^a			phase II ^b			phase IV ^c			phase Y ^d		
	d	(hkl)	Δd	d	(hkl)	Δd	d	(hkl)	Δd	d	(hkl)	Δd
11.68 × 0.01	13.03	(100)	1.35	11.62	(010)	0.06	11.74	(010)	0.06	11.96	(100)	0.28
6.64 ± 0.06	6.62	(020)	0.02	6.90	(0 $\bar{1}$ 0)	0.26	6.56	(110)	0.08	6.96	(020)	0.32
5.86 ± 0.05	5.84	(210)	0.02	5.81	(020)	0.05	5.87	(020)	0.01	5.98	(200)	0.12
5.33 ± 0.03	4.64	(220)	0.69	5.81	(0 $\bar{2}$ 0)	0.05	5.87	(0 $\bar{2}$ 0)	0.01			
3.97	4.13	(310)	0.16	5.10	(220)	0.23	5.26	(2 $\bar{1}$ 0)	0.07	5.50	(210)	0.17
				3.95	(230)	0.02	3.92	(030)	0.05	3.99	(300)	0.02
							3.92	(0 $\bar{3}$ 0)	0.05			
$\Sigma \Delta d $			2.24			0.62			0.27			0.91

^a Phase I: $a = 13.41$ Å, $b = 13.23$ Å, $c = 13.81$ Å, $\beta = 103.72^\circ$. ^b Phase II: $a = 12.17$ Å, $b = 12.58$ Å, $c = 8.64$ Å, $\alpha = 96.28^\circ$, $\beta = 95.03^\circ$, $\gamma = 67.86^\circ$. ^c Phase IV: $a = 10.83$ Å, $b = 13.12$ Å, $c = 9.96$ Å, $\alpha = 72.28^\circ$, $\beta = 77.25^\circ$, $\gamma = 104.48^\circ$. ^d Phase Y: $a = 13.85$ Å, $b = 13.92$ Å, $c = 15.14$ Å, $\beta = 120.22^\circ$. ^e Weak diffraction rings.

Table III. X-ray Diffraction Data for OTiPc^a Films of Various Thicknesses

film thickness (Å)	$2\theta^b$	peak rel intensity	film thickness (Å)	$2\theta^b$	peak rel intensity
8 000	13.1	25	8 000	26.3	100
12 000	12.9	18	12 000	26.2	100
13 000	13.0	15	13 000	26.2	100
16 000	12.7	87	16 000	26.1	100
20 000	12.7	100	20 000	26.3	25
16 000	24.4	69	8 000	28.6	8
20 000	24.5	39	12 000	28.6	6
16 000	25.6	54	13 000	28.7	6
20 000	25.5	68	16 000	28.6	27
			20 000	28.7	52

^a OTiPc was sublimed at 360 °C on glass substrates. ^b 2θ was scanned between 5 and 60°.

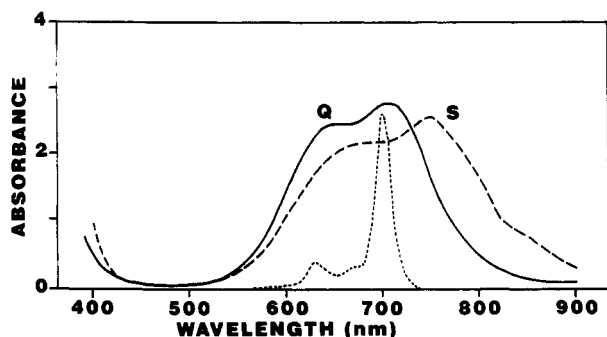


Figure 11. Absorption spectra of two 1300-Å-thick films of the Q type (—) or the S type (---). The absorption spectrum of OTiPc in solution in chloronaphthalene is also given (in arbitrary units).

by a strong absorption with a maximum at 698 nm and two minor vibronic transitions at 627 and 666 nm. The position of the maximum may vary from 685 to 705 nm, depending upon the dipole moment of the solvent used.⁴⁷ Figure 11 also displays the absorption spectrum of both films, Q and S, which have been demonstrated to be amorphous and partially crystalline, respectively. In the solid state, the absorption spectrum of amorphous OTiPc (Q) appears as a simple broadening of the solution spectrum. However, when the film is partially crystalline (S), the maximum of the spectrum moves to the neighborhood of 750 nm and a shoulder appears in the NIR between 800 and 900 nm. This shoulder seems to grow at the expense of the amorphous material absorbing mostly between 600 and 700 nm. As was seen previously, another way to obtain a more crystalline material is to increase the

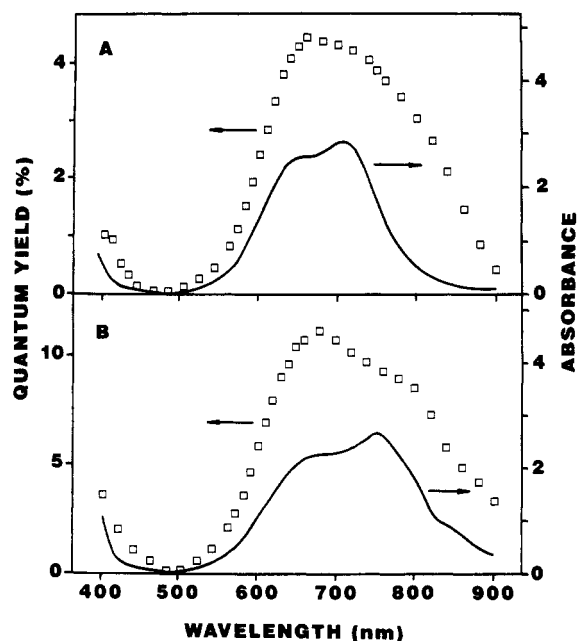


Figure 12. Comparison of absorption (—) and action spectra (□) for two 1300-Å-thick films of the Q type (a) or the S type (b).

thickness of the film by increasing the deposition time. When this is done, the NIR absorbance becomes more important as the film becomes thicker and the Q band becomes larger. However, thicker films become rapidly too absorbing and their optical spectra cannot be measured with accuracy anymore. An absorption in the NIR is therefore characteristic of the crystalline material. Since the molecules are identical in all films, changes in the absorption spectrum have to be attributed to changes in the interactions between the molecules. They can be explained in the frame of the Davydov theory.⁴⁸⁻⁵¹ The appearance of a NIR absorbance means that the molecules are coplanar and in a slipped stacked arrangement. This is in agreement with the deduced crystal structure.

Parts a and b of Figure 12 display the absorption (full line) and action (□) spectra of films Q and S, respectively. Both action spectra have been recorded in short circuit conditions and with the light incident on the film. From these figures, it can be concluded that the action spectra

(48) Kasha, M. In *Spectroscopy of the excited state*; Di Bartolo, B., Ed.; Plenum Press: New York, 1976; p 337.

(49) Kasha, M.; Rawls, H. R.; Ashraf El-Bayoumi, M. *Pure Appl. Chem.* 1965, 11, 371.

(50) McRae, E. G.; Kasha, M. In *Physical Processes in Radiation Biology*; Academic Press: New York, 1964; p 23.

(51) Kasha, M.; Ashraf El-Bayoumi, M.; Rhodes, W. *J. Chim. Phys.* 1961, 58, 916.

(46) Edwards, L.; Gouterman, M. *J. Mol. Spectrosc.* 1970, 33, 292.

(47) Harazone, T.; Takagishi, I.; Matsuzaki, T. *Anal. Sci.* 1991, 7 (Suppl. Proc. Int. Congr. Anal. Sci. 1991, Part 2), 1301.

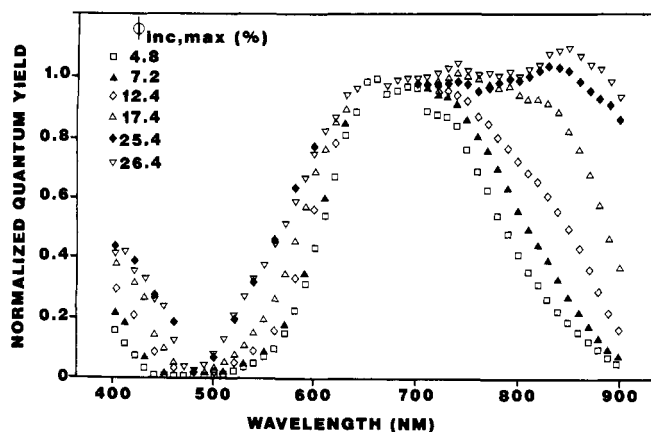


Figure 13. Action spectra, normalized at 660 nm for films of various thicknesses of OTiPc, sublimed at 360 °C during various sublimation periods (\square 1.75; \blacktriangle 2.75; \diamond 4.25; \triangle 7.5; \blacklozenge 20; ∇ 30 min).

follow, in both cases, the absorption spectra reasonably well and that the film with improved crystallinity (S) is much more photoactive than the amorphous one (Q). The quantum yield data displayed in Figure 12a,b are the number of electrons collected per 100 photons incident on the film (ϕ_{inc}).

Figure 13 presents the quantum yields, normalized at 660 nm for films of various thicknesses of OTiPc, sublimed at 360 °C. The thinnest film (\square) was obtained after 1.75 min of sublimation. It is characterized by the morphology of Figure 6a and is amorphous. The thickest film (∇) was obtained after 30 min of sublimation. It is characterized by the morphology of Figure 6c. Among all films which are partially crystalline, it is the one displaying the largest platelets. As can be seen from Figure 13, the main difference between these action spectra is the contribution in the NIR. It increases as the platelets grow in size and this is going along with a drastic improvement of the maximum quantum yield (reported on the graph). Indeed, $\phi_{inc,max}$ rises from 4.8 to 26.4% as the normalized value of ϕ_{inc} at 850 nm rises from 0.1 to 1.1. Films of sublimed OTiPc are therefore made of an amorphous fraction (which may be up to 100% for thin films) characterized by a low photoactivity and a crystalline fraction (whom importance increases with the thickness of the film) characterized by a high photoactivity. Two distinct phases of OTiPc with different absorbance maxima at ca. 720 and 820 nm have already been mentioned by Klofta et al.⁴⁰ After annealing the OTiPc sublimed on a microcircuit, Sims et al.¹⁰ report the appearance of a NIR absorbance and the increase of the photoconductivity by a factor of 50–100 over that in the unannealed films.

In order to obtain action spectra like the ones depicted in Figures 12 and 13, efficient energy transfer has to occur from the amorphous phase to the crystalline one, when both phases coexist. If such was not the case, one would expect low quantum yields in the 600–700-nm region where the amorphous phase mostly absorbs and much larger quantum yields in the NIR, a wavelength range typical of the crystalline material. Exciton generation therefore occurs in both amorphous and crystalline phases of OTiPc, but charge generation happens only in the crystalline phase of the pigment.

Figure 14a presents the action spectra of an amorphous OTiPc film recorded for front side (FS) and back side (BS) illumination. The film is 400 Å thick and obtained

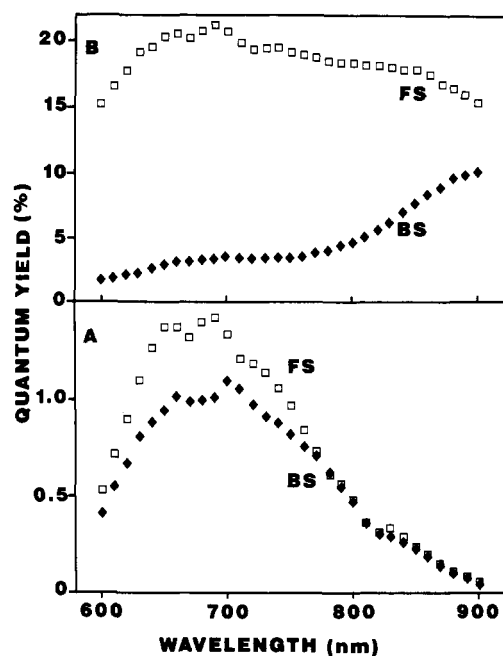


Figure 14. Quantum yields for back (\diamond) and front side (\square) illuminations for amorphous 400-Å-thick (a) or partially crystalline 5000-Å-thick (b) OTiPc films.

by sublimation at 360 °C. With an absorption coefficient of $2 \times 10^5 \text{ cm}^{-1}$ at 705 nm, a filtering effect is already expected for such a thickness since at 705 nm, more than 60% of the light is absorbed in the pigment layer. However, both FS and BS action spectra are similar in shape. This is expected when the film is porous since the electrolyte has access to most of the surface of the pigment aggregate. Such behavior has already been discussed for perylene derivative films, for instance.^{52,53} The only difference between FS and BS spectra is the relative value of their quantum yields. Since the redox has to diffuse in an out of the pores, a reduction of the photocurrent, due to mass transfer limitation of the redox, is expected for BS illumination.

More surprising are the FS and BS action spectra reported in Figure 14b for a thick film (about 5000 Å) of OTiPc obtained by sublimation at 360 °C. The NIR contribution to the FS spectrum indicates that the film contains an important crystalline fraction. On the basis of Figure 7, one might expect that such film has little or no porosity. However, the behavior of both FS and BS spectra in the 600–700-nm region is identical. The only way to explain the BS spectrum is to assume that (i) thick films are still porous and (ii) are more crystalline near the substrate than further away from it. This is a logical assumption since the outside layer of the film has been exposed to annealing temperatures, during the sublimation, for a shorter time than the layer near the substrate. If both assumptions hold, the BS action spectrum corresponds to the absorption spectrum of purely crystalline OTiPc. It is, however, somewhat distorted since the maximum in NIR is not at 850 nm as expected from Figure 13. This can be understood in terms of mass transport limitation of the redox in the solution infiltrated between the grains of the film. Indeed, if the absorption at 900 nm

(52) Danziger, J.; Dodelet, J. P.; Armstrong, N. R. *Chem. Mater.* 1991, 3, 812.

(53) Tamizhmani, G.; Dodelet, J. P.; Côté, R.; Gravel, D. *Chem. Mater.* 1991, 3, 1046.

in the crystalline region is lower than at 850 nm, photons will be able to reach further away from the substrate, before being completely absorbed. A somewhat larger current is therefore expected at 900 nm since the transfer of the photogenerated electron will then happen closer to the surface of the film than at 850 nm, where more I_3^- anions should be available. If this rationalization is correct, one realizes that crystalline OTiPc has an absorption shoulder in the 700-nm region, reinforcing the possibility of the proposed energy transfer from the amorphous to crystalline regions in the layer.

Conclusion

When OTiPc is sublimed on SnO_2 or glass, the physical and photoelectrochemical properties of the films are determined by the temperature reached by the substrate during the sublimation. Amorphous films are obtained for substrate temperatures below about 80 °C while partially crystalline films are obtained when the substrates are allowed to reach about 140 °C.

Partially crystalline films are the only ones to absorb in the NIR. This typical absorption is going along with an improvement of the photoactivity. For instance, for films of the same thickness (1300 Å), the maximum quantum yield is about 2–4 electrons/100 incident photons for the amorphous films; it is 12 for the partially crystalline ones. The dominant OTiPc polymorph in the latter films is not the same for all films thicknesses. It is phase IV OTiPc

for thin films (≤ 2000 Å), as deduced by TEM, but becomes phase I, as deduced by XRD, for films ≥ 8000 Å. Quantum yields up to about 25% have been observed for such films. They display a peak at 850 nm in their action spectra and a 1.5 mA cm^{-2} of short circuit photocurrent under polychromatic illumination. As the dominant polymorphic species probably changes gradually from phase IV to phase I, there is no drastic change in the photoactivity when the thickness of the film increases.

A NIR absorbance is one of the factors that is required to reach high photoactivities. However, it is not the only one. Adequate O_2 doping is equally important as it is demonstrated by a difference of a factor 3 between short circuit photocurrents characterizing OTiPc films grown, in the same conditions, from powders purified by sublimation in lower (10^{-2} Torr) or higher ($\leq 10^{-5}$ Torr) vacuum.

Dark and photoconductivity measurements at various temperatures are now undertaken in order to define the eventual influence of O_2 and the crystallinity of OTiPc on its charge carrier densities and mobilities. Surface sensitive techniques like XPS and SIMS time of flight will also be used to investigate in greater details the exact nature of oxygen interaction with this material.

Acknowledgment. This work was supported by NSERC. Ph.G. thanks Prof. J. M. Streydio from UPCIM, Université Catholique de Louvain (Belgium) for making his research studentship possible at INRS.